Interface structure of (001) and (113)*A* GaAs/AlAs superlattices

D. Lüerßen, A. Dinger, and H. Kalt
Institut für Angewandte Physik, Universität Karlsruhe, D-76128 Karlsruhe, Germany

W. Braun, R. Nötzel, and K. Ploog
Paul-Drude-Institut für Festkörperelektronik, D-10117 Berlin, Germany

J. Tümmler and J. Geurts
I. Physikalisches Institut, RWTH Aachen, D-52056 Aachen, Germany
(Received 17 December 1996; revised manuscript received 7 August 1997)

The interfaces of short-period GaAs/AlAs superlattices grown on GaAs (001) and (113)*A* surfaces are investigated by means of reflection high-energy-electron diffraction (RHEED) and Raman spectroscopy. RHEED investigations during growth of the heterostructures reveal an intermixed normal (AlAs-on-GaAs) interface while the inverted one is seen to be abrupt. We measured the Raman shifts of the GaAs-like confined optical phonons. In [001] grown superlattices, we determine the thickness of the intermixed region at the normal interface by comparison of the phonon wave vectors with the dispersion curve. This procedure is also applied to the [113] grown samples, where a splitting of the confined LO_3 modes confirms the presence of an interface corrugation. We determine the height of the corrugation to be 3.4 Å (two bilayers) at one interface while the other one is intermixed. This model is used for a reinterpretation of previously published Raman data [da Silva *et al.*, Phys. Rev. B **53**, 1927 (1996)] leading to a better agreement between experiment and theory. [S0163-1829(98)10003-6]

I. INTRODUCTION

Since the report of a self-ordered corrugation in GaAs/AlAs superlattices grown on the GaAs (113)*A* surface by Nötzel and co-workers,[1,2] these structures have been of great research interest due to the expected quantum-wire-like properties.[3–8] However, the corrugation is not intrinsic to this growth direction but depends strongly on the growth conditions so that even flat surfaces can be achieved.[9] Nevertheless, in the case of corrugated surfaces the lateral 32-Å period of the reconstruction that is obtained under usual As-rich conditions is widely accepted. The height of the structure was first determined to be 10.2 Å [six bilayers (BL)] (Refs. 1,2), but it was recently confirmed to be only 3.4 Å (2 BL) using scanning tunneling microscopy[10] and kinematic modeling of experimental reflection high-energy electron diffraction (RHEED) data.[11]

The RHEED method is well suited to study semiconductor surfaces and their reconstruction during growth by molecular-beam epitaxy (MBE). The diffraction pattern directly reflects the reconstruction, whereas temporal intensity modulations are correlated to the coverage of the topmost bilayer. Since it is an *in situ* method, one can investigate whether the reconstruction is preserved during heteroepitaxy.

Since the so far mentioned techniques study *surfaces*, different methods must be applied to investigate the *interfaces* of heterostructures. This has been done, e.g., by optical anisotropy measurements,[12,13] which excluded the 6-BL interface corrugation. Also, the frequency of confined optical phonons is sensitive to the layer thickness in quantum wells or superlattices.[14] Raman spectroscopy can, therefore, reveal details on thickness fluctuations with a lateral length scale larger than some critical length.[15,16] This situation applies to thin corrugated superlattices (CSL's). Recently, Raman studies on confined optical phonons in CSL's have been interpreted in terms of a corrugation of two bilayers at both interfaces (Fig. 1, left part).[17] This interpretation will be called in the following the *antiphase corrugation* (APC) model.

In this paper, we show that the assumption of one corrugated and one intermixed interface (Fig. 1, right part) leads to a better agreement with the experimental data than the APC model. We will call the former assumption *corrugated and intermixed interface* (CII) model. This approach is based on RHEED and Raman investigations of both, [001] and [113] grown GaAs/AlAs superlattices. The interpretation of the Raman experiment is based on the calculations of Molinari *et al.*,[18] which describe the penetration of the confined optical phonons into intermixed interface regions. Additionally, recent transmission electron microscopy (TEM) studies of (001) GaAs/AlAs superlattices[19] and Raman data from Ref. 17 will be included in the discussion.

This paper is organized as follows: first, details on the

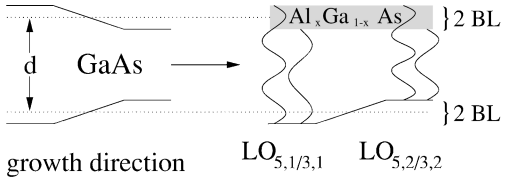

FIG. 1. Left-hand side: antiphase corrugation (APC) model used in Ref. 17. Right-hand side: Schematic model for the corrugation with intermixing at one interface (CII). The penetration depth of the LO_3 and LO_5 confined modes are indicated for clarification. Intermixing leads to a 2-BL difference in the well width felt by different confined phonon modes.

investigated samples and on the experimental setup will be given. Based on the finding of asymmetric Ga segregation in RHEED measurements on (001) superlattices, we use Raman spectroscopy to determine an effective layer thickness and, therefore, also the thickness of the alloyed region at the AlAs-on-GaAs interface (Sec. III). In the next section (Sec. IV A) we will show by means of RHEED that a similar asymmetric segregation takes place in (113)*A* superlattices. Raman investigations further prove that the corrugation is preserved at only one interface (Sec. IV B). We will close the article with a summary (Sec. V).

II. SAMPLES AND EXPERIMENTAL DETAILS

Our (001) and (113)*A* samples were grown simultaneously by pulsed growth MBE, i.e., with a growth interruption of typically 30 s at each heterointerface. After oxide desorption at 580 °C, growth was typically initiated at 550 °C. Then the sample was heated to approximately 600 °C, which was found from the relative maximum of the RHEED intensity oscillation amplitude to be the optimum growth temperature. The growth rates were 0.6 to 0.8 μm/h. RHEED was used to adjust the As_4 pressure so that the 8 $\times$1 surface reconstruction of the (113)*A* surface, which corresponds to the corrugated surface, was maintained during growth. The sample misorientation was less than 0.1° for both orientations. *In situ* RHEED experiments were performed at incidence angles around 1° using an electron energy of 20 keV.

Samples with different layer thicknesses were investigated, and we will discuss the Raman data of two selected (001)/(113)*A* pairs of samples in detail. The [001] layer thickness of the $(GaAs)_8/(AlAs)_8$ sample is (23 Å/22 Å) with 180 periods. The $(GaAs)_{11}/(AlAs)_{10}$ sample has a thickness of (30 Å/28 Å) and 140 periods. The layer thicknesses given by the growth rates were confirmed by x-ray diffraction. For both (001) superlattices (SL's) and (113)*A* CSL's, the thicknesses will be given in Å, e.g., 23/22 SL or 23/22 CSL for the first samples. This notation is unambigous since the layer thickness of both types of superlattices is equal when grown simultaneously, but not the number of bilayers in growth direction.

The Raman measurements were carried out at 80 K using the 4880 Å line of an Ar^+ ion laser, which means off-resonant excitation, and a SPEX 1403 double grating spectrometer with a multichannel detection resulting in a resolution of about 1 cm^{-1}. All spectra were recorded in quasibackscattering geometry, i.e., with an angle of about 20° between incident laser beam and the surface normal. Typical Raman spectra for (001) and (113)*A* oriented samples are shown in Fig. 5.

For the (001) oriented sample [Fig. 5(a)], a spectrum in the scattering geometry in which the odd-numbered confined LO-phonon modes are symmetry allowed is shown. In the $[001]([\bar{1}00][100])\overline{[001]}$ scattering geometry the even-numbered modes can be measured. The resulting phonon energies will be used in the following discussion, although no spectrum is explicitly shown. A possibly observable splitting of higher LO phonon modes in (113)*A* SL's with corrugated interfaces can be resolved in the $[113]([33\bar{2}][\bar{3}3\bar{2}])\overline{[113]}$ scattering geometry[17] [Fig. 5(b)].

III. ASYMMETRIC INTERFACE INTERMIXING IN (001) SUPERLATTICES

Segregation of group-III atoms at heteroboundaries can be investigated, e.g., by *in situ* electron spectroscopy methods.[20] Recently, reconstruction-induced phase shifts (RIPS) of RHEED intensity oscillations have been used to study the interface structure of (001) GaAs/AlAs SL's.[21] These experiments reveal a significant segregation of Ga at the normal (AlAs-on-GaAs) interface, whereas an abrupt inverted (GaAs-on-AlAs) interface is found. Ga can still be detected typically 6–8 BL away from the nominal interface position. This does not imply that the intermixing degree is high that far away from the nominal heteroboundary. The actual effective thickness of the intermixed region cannot be deduced from the RHEED data since the diffraction pattern is not only sensitive to the surface reconstruction, but also to the density of terraces or steps. Therefore, quantitative measurements are difficult. We will determine the intermixed-layer thickness by the Raman measurements described below. TEM measurements confirm the asymmetric segregation of Ga at the heterointerfaces.[19]

The asymmetric segregation seems not to depend significantly on surface reconstruction and morphology, since a fractional layer of Sn floating on the surface during interface formation does not change the segregation behavior, although it completely changes the surface structure.[22] This independence of the growth details indicates a thermodynamically driven process. The different bond enthalpies of AlAs compared to GaAs (202.9 kJ mol^{-1} and 209.6 kJ mol^{-1}, respectively[23]) favor the incorporation of Ga in AlAs, while having a demixing effect for the other combination. Generalizing this idea, the asymmetric segregation behavior should also be maintained during growth on different crystal surfaces such as (113)*A*. This assumption is confirmed in Sec. IV.

We will now use Raman spectroscopy of confined optical phonons to investigate the effective thickness of the intermixed layer at the normal interface. The phonons confined in the GaAs well have effective wave vectors $q_s=(s\pi)/(d+\delta)$ where s is the order of the confined mode, d is the thickness of the well seen by the phonon, and $0<\delta<1$ is a phenomenological parameter characterizing the penetration length of the confined mode into the barrier. This δ is usually assigned to the As layer common to both GaAs and AlAs which effectively increases the layer thickness. Since intermixing of an interface leads to a modification of the effective well width,[18] we will keep $\delta=0$ and only modify the effective well width to fit the experimental data of the confined modes.

Intermixing effects have been studied theoretically, e.g., by Jusserand[15] and by Molinari *et al.*[18] Molinari *et al.* did the calculations especially for (001) GaAs/AlAs SL's in relation to Raman spectroscopy. The intermixing was assumed to be identical at both interfaces, and the intermixed regions were treated as $Al_{0.5}Ga_{0.5}As$ mixed cystals. The essential result is the following: phonon modes with a high energy cannot penetrate into the disordered region whereas those with lower energy can. The effective well width can, therefore, differ for different confined phonon modes. This can be easily understood: the whole dispersion curve of the GaAs-like LO-

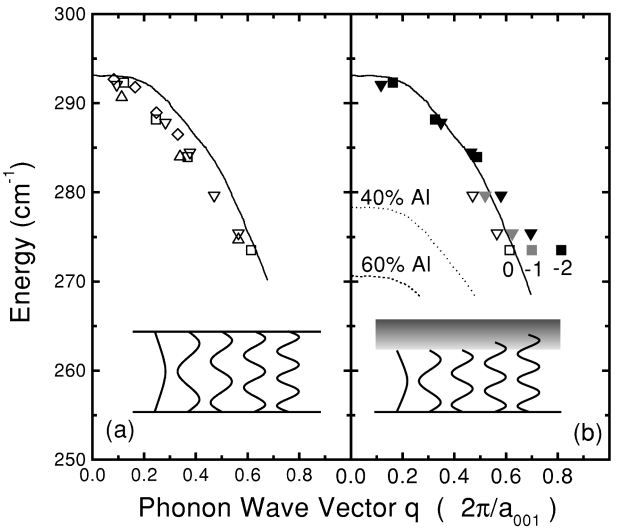

FIG. 2. GaAs LO-phonon [001] dispersion with confined mode frequencies for 23/22 SL (□), 30/28 SL (▽), 25/40 SL (△), and 34/26 SL (○). The effective wave vectors have been calculated in (a) using a constant GaAs well width, while in (b) an energy-dependent penetration into an intermixed heteroboundary is applied. The difference between open, gray, and black filled symbols equals 1 BL. The sketch illustrates the modes applicable for the 30/28 SL.

phonon mode is shifted towards lower energies in $Al_xGa_{1-x}As$ relative to its value in GaAs. This is illustrated in Fig. 2(b) for an Al content of 40% and 60%,[24] respectively. For energies in the region where the dispersion curves of GaAs and $Al_xGa_{1-x}As$ do not overlap, the barrier for the GaAs confined modes consists of AlAs at the inverted interface and of $Al_xGa_{1-x}As$ at the normal interface. For energies below some critical wave number the $Al_xGa_{1-x}As$ region belongs to the well, and the barrier consists of AlAs on both interfaces.

Now we will apply these ideas to determine the effective well thickness in the (001) superlattices. Figure 2 shows the known LO-phonon dispersion relation for bulk GaAs (Ref. 25) together with experimentally determined phonon mode energies for several samples. The wave vectors in (a) are calculated for the average layer thicknesses obtained by x-ray diffraction. Obviously, all data points are shifted towards lower **q** values relative to the dispersion curve. It means that the confined LO phonons feel a reduced GaAs well thickness compared to the data obtained by x-ray diffraction. Having the RHEED analysis in mind, this behavior is expected since this determination of the wave vectors does not take into account that the effective well thickness seen by the confined phonons is modified (i.e., reduced) due to intermixing of the normal interface.

In order to determine explicitly the effective well width of the 23/22 SL and 30/28 SL, we change the thickness that is used for the calculation of the phonon wave vectors in units of 1 BL. The phonon energies are fixed and given by the experimental values. Then we compare the resulting wave vector—energy pairs with the dispersion curve [Fig. 2(b)]. For the open symbols, we calculated the wave vectors with the nominal layer thicknesses, for the gray and the black ones the effective well width has been reduced by 1 and 2 BL, respectively. For the phonon modes with wave numbers down to ≈ 285 cm^{-1} the black data points are in very good agreement with the dispersion curve. Thus we can conclude that intermixing reduces the effective GaAs well width by 2 BL. For modes with lower energies, penetration into the intermixed region becomes important. This is expected since here the GaAs LO-phonon dispersion in GaAs begins to overlap with the GaAs-like one in $Al_xGa_{1-x}As$ with a reasonably high Al content. With rising mode order the penetration depth increases, as is illustrated in the inset of Fig. 2 for the case of the 30/28 SL (▽). This behavior is reflected in the fact that on the one hand the black data points increasingly deviate from the dispersion. On the other hand, good agreement is again achieved if a penetration of the order of 1 (gray symbols) or 2 BL (open symbols) into the intermixed region is introduced.

To summarize this section, from the interpretation of RHEED we know that the normal interface is intermixed and the inverted one is abrupt. Applying this to the interpretation of Raman measurements, we determine the effective width of the GaAs well for the GaAs-like confined LO-phonon modes in (001) superlattices. We will now study the interface structure in the more complex [113]-oriented corrugated superlattice system.

IV. INTERFACE INTERMIXING AND CORRUGATION IN (113)*A* SUPERLATTICES

A. RHEED investigations in pulsed growth MBE

The problem in investigating the (113)*A* SL's by means of the RIPS is the fact that the GaAs, the AlAs, and the $Al_xGa_{1-x}As$ surfaces show the same reconstruction (in Fig. 3 for a sample slightly misoriented towards the screen). This means that there cannot be a phase shift due to the change in surface reconstruction at the heterointerface. The usual approach of evaluating the oscillation phase is, therefore, not practicable. In addition, no RHEED intensity oscillations are observed for AlAs homoepitaxy on this surface. We therefore have to resort to the measurement of absolute RHEED intensities.

A typical pulsed RHEED measurement is shown in Fig. 4 with the measurement geometry included in the inset. For GaAs homoepitaxy and at the beginning of AlAs heteroepitaxy, oscillations are observed. These could only be found at low incidence angles at the marked position. This position corresponds to a forbidden reflection in the kinematically simulated diffraction diagram of the surface structure,[11] confirming the multiple scattering nature of the diffraction process leading to oscillations.

For our purpose, however, the average diffracted intensity during the sequence is more interesting. It remains almost constant during the GaAs cycles, where pronounced oscillations can be seen at the beginning of each pulse. We can, therefore, be sure that the surface smoothes during the growth interruptions. During the growth of AlAs, the situation is much different: the average intensity rises slowly and is still gaining during the third pulse. Furthermore, the intensity level shows a memory effect after the growth interruptions. Therefore, it cannot be a measure of the surface roughness, since the surface smoothes during the recovery period. For this reason, we can correlate the average intensity to the

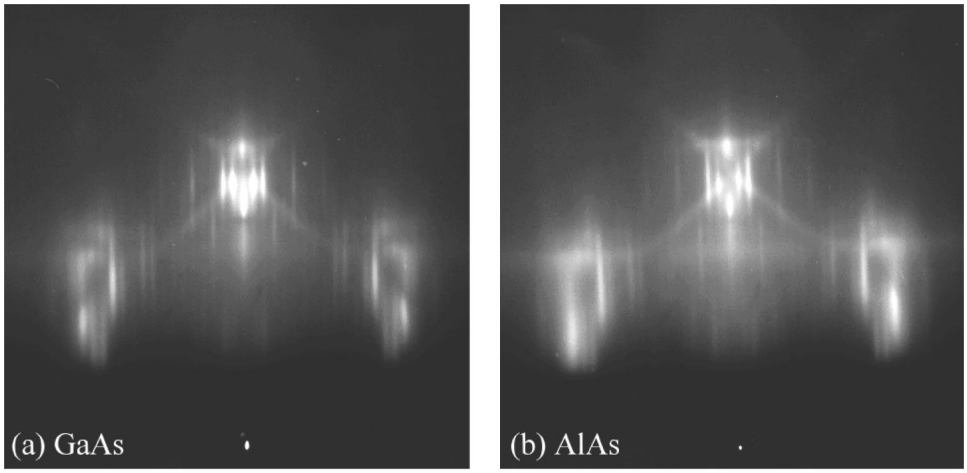

FIG. 3. RHEED patterns for (a) the GaAs and (b) the AlAs (113)*A* crystal surface along $[33\overline{2}]$. The sample temperature was 605 °C using 20 keV electrons at an incidence angle of 1.2°. The sample is miscut by 0.9° towards the screen.

material composition. At the beginning of GaAs heteroepitaxy (at 300 s in Fig. 4), the intensity change is fast, similar to the observed phase change in RIPS on (001) superlattices.

Interpreting the RHEED average intensity as a measure for material composition, we observe a relatively slow decreasing Ga content for growth of AlAs on GaAs, while the GaAs-on-AlAs interface is sharp. The intensity during AlAs growth does not saturate even after the third pulse (corresponding to 40-Å layer thickness), whereas it reassumes the GaAs value basically during the first GaAs bilayer. This allows us to conclude that, similar to the (001) orientation, there is strongly asymmetric Ga segregation for the (113)*A* interfaces. This implies that the normal interface is intermixed, whereas the inverted interface is abrupt. The intermixing does not affect the surface reconstruction. The latter is maintained throughout growth, which is proved by the constant RHEED pattern.

Since the RHEED experiments show that one interface is abrupt while there is Ga segregation at the other one, we propose the following interface structure: the distribution of the group-III atoms has a corrugationlike profile at the inverted interface and is smeared out at the normal interface. We will test this proposal by Raman investigations in the following section.

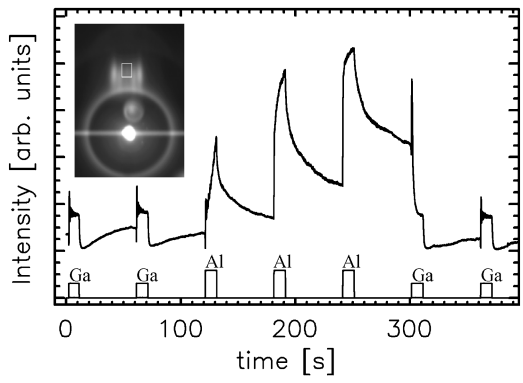

FIG. 4. RHEED intensity evolution for a GaAs-AlAs pulsed growth sequence on (113)*A* along the $[33\overline{2}]$ azimuth. The measurement geometry is shown in the inset. The electron energy was 20 keV with an incidence angle of 0.7°. The sample temperature was 602 °C using an As_4 pressure of 1.7×10^{-3} Pa. The growth rates were 1.5 Å/s for GaAs and 1.3 Å/s for AlAs.

B. Raman studies of confined optical phonons and discussion of the interface models

If there were a corrugated interface, one should ask if confined optical phonons averaged over this structure. A criterion similar to confinement of electrons in a steplike heterostructure can be examined:[15,16]

$$\lambda_c = \frac{d\sqrt{m_z/m_{xy}}}{s\sqrt{2\Delta d/d}},$$

where d is the layer thickness, Δd is the height of the corrugation, s is the order of the confined mode, and m_z, m_{xy} are the masses in growth direction and perpendicular to it, respectively. It is reasonable to assume an isotropic phonon mass, which is the curvature of the phonon dispersion at the Γ point. For relevant layer thicknesses and mode order $s \geqslant 3$ the critical length λ_c is smaller than the period of the corrugation (32 Å). We should, therefore, be able to observe a splitting of the confined LO modes with order 3 and higher, which is due to different phonon wave vectors **q** corresponding to different layer thicknesses (Fig. 1, right part).

We will now discuss the Raman spectrum for the 23/22 CSL plotted in Fig. 5(b). It was recorded in the $[113]([33\overline{2}][33\overline{2}])[\overline{113}]$ scattering geometry in which LO-phonon scattering is only weakly allowed. A splitting of the LO_3 phonon is clearly observable, the peaks are labeled $LO_{3,1}$ and $LO_{3,2}$, respectively. We can exclude that the second peak is a LO_5 mode because the resulting **q** vector would be far too large to be compatible with the phonon dispersion. Different layer thicknesses can be excluded by a comparison with the properties of the simultaneously grown [001]-oriented superlattice. Its Raman spectrum in the $[001]([100][010])[\overline{001}]$ scattering geometry [Fig. 5(a)] exhibits a small linewidth of the LO_1-phonon mode (2 cm^{-1}) and shows no splitting of the LO_3 mode. We can conclude that there is only one GaAs layer thickness inside the sample.

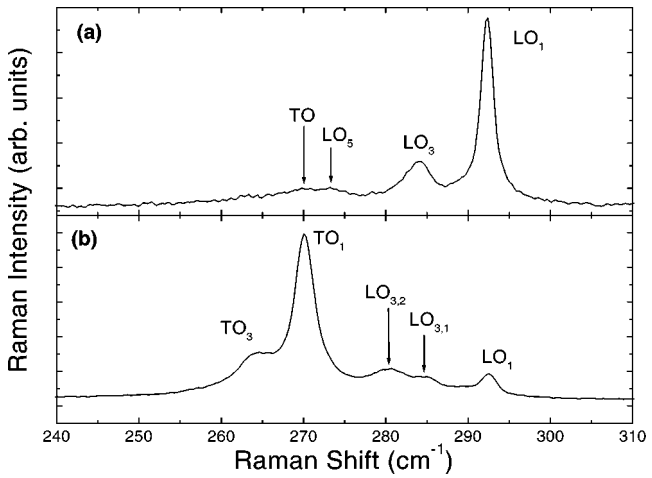

FIG. 5. Raman spectra for the 23/22 SL (a) and 23/22 CSL (b) in the $[001]([100][010])\overline{[001]}$ and $[113]([33\bar{2}][3\bar{3}2])\overline{[113]}$ scattering geometries, respectively. In (b), the splitting of the LO_3 mode can be clearly observed.

This fact is also proved by photoluminescence and photoluminescence excitation measurements (not shown here). The spectrum of the CSL [Fig. 5(b)] shows the TO_3 confined mode which was not resolved so clearly in previously published Raman data.[26–28] Summarizing these facts, the samples are of good quality. The splitting of the confined LO_3 and deviations of the confined modes from the dispersion relation will, therefore, have their origin in the interface properties of the sample under investigation. The 30/28 CSL has very similar properties in Raman spectroscopy.

We will now use the different interface models to calculate the wave vectors in growth direction and compare the resulting data points with the dispersion relation. Figure 6 shows these data points for the 23/22 CSL [part (a), □, and ■] and 30/28 CSL [part (a), ▽, and ▼]. Previously published data from Ref. 17 are given in Fig. 6(b) (○ and ●). In

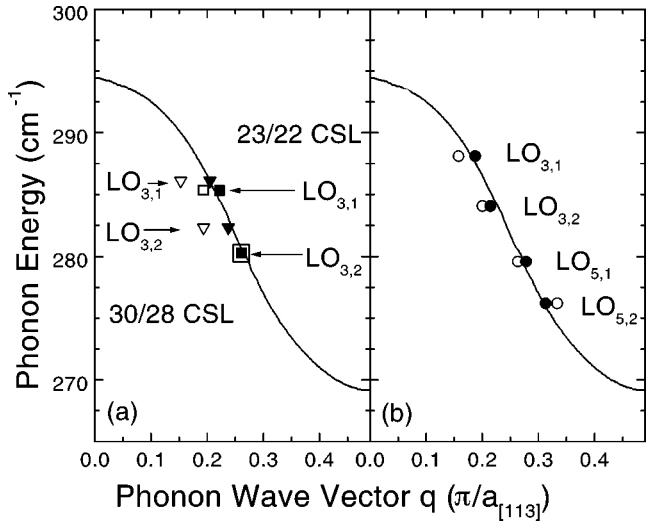

FIG. 6. GaAs LO-phonon dispersion relation in the [113] direction together with the data points for the splitted modes in (a) the 23/22 CSL (□, ■) and the 30/28 CSL (▽, ▼) and (b) for the data of Ref. 17 (○, ●). The open symbols indicate the APC model; the full ones belong to the CII model for the interface structure.

all cases, the open symbols represent analysis according to the APC model (Fig. 1, left part), whereas the wave vectors for the filled symbols have been calculated by means of the CII model (Fig. 1, right part).

In the APC model, there are no degrees of freedom. On the other hand, there is one parameter in the CII model that is the effective reduction of the GaAs well width. In the APC model, the data points have a fixed place in the wave vector–energy diagram. The determination of the effective GaAs well width in the CII model is achieved by shifting the data points on the q axis onto the dispersion curve. However, this method is not arbitrary since the relative distance on the q axis for the splitted modes is fixed in the model.

The results of the analysis in the case of the 23/22 CSL and the 30/28 CSL are the following (see Fig. 6): first, the relative distance on the q axis agrees with a 2-BL corrugation at one interface for both samples. This can be most easily verified in the case of the 23/22 CSL, where the $LO_{3,2}$ data points coincide for both the APC and the CII model, but the wave vectors for the $LO_{3,1}$ mode differ. The wave-vector calculation in terms of the CII model fits better to the theoretical prediction. Second, the LO_3 modes feel a reduction of the GaAs layer by 1 BL and 4 BL for the 23/22 CSL and the 30/28 CSL, respectively. The strong deviation of the data points from the dispersion relation in case of the 30/28 CSL using the APC assumption cannot be explained within the frame of this model. These two facts favor the CII model over the APC model.

The best test for the CII model is expected from the data of Ref. 17, since in this case phonons in a wider energy range are found [see Fig. 6(b)]. As in the case of (001) grown SL's, we should be able to demonstrate the different penetration of the confined optical phonons into the intermixed region. By calculating the wave vectors according to the APC model, the data points scatter around the dispersion curve. On the other hand, all points fit well in the CII model using 2 BL larger penetration for the LO_5 than for the LO_3 modes, respectively.[29] The difference of the well-width reduction felt by different confined modes is comparable to the amount determined in the case of [001] SL's and seems, therefore, reasonable.

We conclude that the corrugation exists at only one heteroboundary with a height of 2 BL. The deviation from the theoretical prediction is minimized for calculation of the wave vectors using the CII model, and we are able to determine the penetration of the confined modes into the intermixed heteroboundary.

V. SUMMARY

We have shown evidence by means of RHEED and Raman spectroscopy that in (001) and (113)*A* GaAs/AlAs superlattices the inverted interface is sharp while the normal one is intermixed. Splittings in higher-order odd LO modes in (113)*A* grown samples show that one interface is corrugated with a corrugation height of 2 BL (3.4 Å). We are able to determine the penetration of the confined phonon modes into the intermixed interface regions.

[1] R. Nötzel *et al.*, Phys. Rev. Lett. **67**, 3812 (1991).
[2] R. Nötzel, N. Ledentsov, L. Däweritz, K. Ploog, and M. Hohenstein, Phys. Rev. B **45**, 3507 (1992).
[3] V. A. Shchukin, A. I. Borovkov, N. N. Ledentsov, and P. S. Kop'ev, Phys. Rev. B **51**, 17 767 (1995).
[4] P. V. Santos *et al.*, Phys. Rev. B **52**, 1970 (1995).
[5] Z. Y. Xu *et al.*, Phys. Rev. B **51**, 7024 (1995).
[6] E. Ribeiro, F. Cerdeira, and A. Cantarero, Phys. Rev. B **51**, 7890 (1995).
[7] A. C. Churchill, G. H. Kim, M. Y. Simmons, D. A. Ritchie, and G. A. C. Jones, Phys. Rev. B **50**, 17 636 (1994).
[8] G. Armelles *et al.*, Phys. Rev. B **49**, 14 020 (1994).
[9] Y. Hsu, W. Wang, and T. Kuan, Phys. Rev. B **50**, 4973 (1994).
[10] M. Wassermeier *et al.*, J. Cryst. Growth **150**, 425 (1995).
[11] W. Braun *et al.*, Appl. Surf. Sci. **104/105**, 35 (1996).
[12] W. Langbein *et al.*, Nuovo Cimento D **17**, 1561 (1995).
[13] W. Langbein *et al.*, Phys. Rev. B **54**, 10 784 (1996).
[14] B. Jusserand, F. Alexandre, D. Paquet, and G. L. Roux, Appl. Phys. Lett. **47**, 301 (1985).
[15] B. Jusserand, Phys. Rev. B **42**, 7256 (1990).
[16] Yu. A. Pusep *et al.*, Phys. Rev. B **51**, 5473 (1995).
[17] S. W. da Silva *et al.*, Phys. Rev. B **53**, 1927 (1996).
[18] E. Molinari, S. Baroni, P. Giannozzi, and S. de Gironcoli, Phys. Rev. B **45**, 4280 (1992).
[19] W. Braun, A. Trampert, L. Däweritz, and K. H. Ploog, Phys. Rev. B **55**, 1689 (1997).
[20] J. M. Moison *et al.*, Phys. Rev. B **40**, 6149 (1989).
[21] W. Braun and K. Ploog, Appl. Phys. A: Solids Surf. **60**, 441 (1995).
[22] W. Braun and K. Ploog, J. Cryst. Growth **150**, 62 (1995).
[23] http://www.shef.ac.uk/~chem/web-elements/chem/As.html.
[24] Z. C. Feng *et al.*, Phys. Rev. B **47**, 13 466 (1993).
[25] D. J. Mowbray, M. Cardona, and K. Ploog, Phys. Rev. B **43**, 1598 (1985).
[26] A. J. Shields *et al.*, Phys. Rev. B **49**, 7584 (1994).
[27] Z. V. Popović *et al.*, Phys. Rev. B **52**, 5789 (1995).
[28] Z. V. Popović *et al.*, Phys. Rev. B **49**, 7577 (1994).
[29] We can only determine the difference in the penetration lengths since da Silva *et al.* determined the layer thicknesses by Raman spectroscopy. Acoording to our previous discussion, a reference measurement is needed.